The Radiopharmaceutical Chemistry of the Radioisotopes of Lutetium and Yttrium

Elaheh Khozeimeh Sarbisheh and Eric W. Price

Fundamentals

The Solution Chemistry of Lu^{3+} and Y^{3+}

To begin our discussion of these versatile radiometals, we will delve into some relevant chemical properties of Lu^{3+} and Y^{3+}. The physiologically relevant oxidation state of yttrium and lutetium is 3+, and these metal ions are redox stable *in vivo*. These 3+ cations are considered hard metal ions with a preference for hard donor atoms such as oxygen and nitrogen [1]. The typical coordination numbers of Lu^{3+} and Y^{3+} are 8 and 9, although 10 is also possible. Furthermore, the effective ionic radius of Lu^{3+} is 98 pm, while that of Y^{3+} is 102 pm [2], and their Pauling electronegativity values are 1.27 and 1.22, respectively [3]. Radiolabeling experiments confirm what these physical properties suggest: radiolabeling conditions and chelator selectivity are effectively the same for $[^{177}Lu]Lu^{3+}$ and $[^{86}Y]/[^{90}Y]Y^{3+}$ ions. Although yttrium is a transition metal, it is often treated as a "pseudo-lanthanide" for the reasons discussed above [4].

The most common coordination geometries for Y^{3+} and Lu^{3+} when bound by chelators are square antiprismatic, distorted square antiprismatic, and monocapped square antiprismatic [5]. The metal ions Y^{3+} (pKa = 7.7) and Lu^{3+} (pKa = 7.6) are not as acidic or prone to hydrolysis as metal ions such as Ga^{3+} (pKa = 2.6) or Zr^{4+} (pKa = 0.22) [6]. However, above pH 3, both Y^{3+} and Lu^{3+} still have a tendency to form insoluble $[M(OH)_3]$ species [7, 8]. As a result, these radiometals are typically formulated in 0.05 or 0.1 M HCl solution to ensure uniform speciation and prevent the formation of insoluble hydroxides. Despite the possibility of forming insoluble hydroxide species above pH 2–4, the buffers used for radiolabeling with Y^{3+} and Lu^{3+} typically reside between pH 4 and pH 6 and, somewhat surprisingly, still work well. This is partially because at very low pH (*e.g.* 1–2), the acidic coordinating groups of chelators (*e.g.* carboxylic acids, pKa ~4–5) may become protonated, a process which can prevent the coordination of the radiometal.

As we embark on our description of the application of these radiometals, we would like to start with an important preface. The chemistry of a radioactive isotope (radionuclide) of an element (*e.g.* yttrium-86 or yttrium-90) is effectively identical to that of its stable, non-radioactive isotopologues (*e.g. yttrium-89*). However, one facet of chemistry that is indeed drastically different when using radionuclides compared to their nonradioactive cousins is that radiochemistry is typically performed under extremely dilute conditions. This extreme dilution partially solves the issue of insoluble hydroxide species that we have discussed. At the concentrations typical for solutions of radiometals, species such as $[M(OH)_3]$—which are normally insoluble—are actually partially soluble. In addition, in radiolabeling reactions, the chelator is present in large molar excess over the radiometal cations (see the section on "Tricks of the Trade: Moles and Specific Activity" for a thought exercise on specific activity). Typically, very small molar quantities of a chelator-vector conjugate (*e.g.* peptide, antibody) are radiolabeled using even smaller molar quantities of radiometal ions. As the radionuclide is essentially always the limiting reagent, a radiolabeling mixture effectively contains a huge excess of unlabeled molecules, with only a small fraction of molecules containing a radionuclide label. Unless the precursor molecule can be separated from the radiolabeled molecule (*e.g.* via chromatography), there will always be a large excess of unlabeled conjugate in the mixture.

Relevant Nuclear Properties of Lutetium and Yttrium Radionuclides

The chart of the nuclides highlights a plethora of radionuclides that have been discovered for both lutetium and yttrium, but only certain nuclides can be produced routinely using existing cyclotron/LINAC/reactor infrastructure and

E. Khozeimeh Sarbisheh · E. W. Price (✉)
Department of Chemistry, University of Saskatchewan, Saskatoon, SK, Canada
e-mail: eric.price@usask.ca

J. S. Lewis et al. (eds.), *Radiopharmaceutical Chemistry*, https://doi.org/10.1007/978-3-319-98947-1_20

Table 1 Relevant nuclear properties of Y^{3+} and Lu^{3+} radionuclides, EC = electron capture [9–11]

Nuclide	$t_{1/2}$ (h)	Decay mode (abundance)	Energy (keV)	Typical production method
[^{177}Lu]Lu^{3+}	159.4	β^- (76%)	γ 112, 208 β^- 177 (12%), 385 (9%), 498 (79%)	^{176}Lu(n,γ)^{177}Lu
[^{86}Y]Y^{3+}	14.7	β^+ (33%) EC (66%)	γ 139–4900 β^+ 1221 (max) β^+ 535 (avg.)	Cyclotron, ^{86}Sr(p,n)^{86}Y
[^{90}Y]Y^{3+}	64.1	β^- (100%)	β^- 2280 (max)	^{90}Zr(n,p)^{90}Y

also possess suitable decay properties for medical applications. For example, a radionuclide such as germanium-68 with a half-life of ~271 days would obviously not be suitable for use inside the human body due to concerns over long-term radiation exposure. However, it may have a compelling use for making a radionuclide generator for a more useful, shorter-lived daughter nuclide (*e.g.* [^{68}Ge]Ge^{4+}/[^{68}Ga]Ga^{3+} generator). As a result, only three nuclides of Y^{3+} and Lu^{3+} have been explored for medical use: yttrium-90 ([^{90}Y]Y^{3+}) for radionuclide therapy, yttrium-86 ([^{86}Y]Y^{3+}) for imaging, and lutetium-177 ([^{177}Lu]Lu^{3+}) for imaging and radionuclide therapy (Table 1) [9–11].

Yttrium-90

Yttrium-90 ($t_{1/2}$ = 64.1 h, $E_{\beta^-(max)}$ = 2280) almost strictly emits β^- (beta) particles and has been clinically used for both radioimmunotherapy (*e.g.* [^{90}Y]Y-Zevalin) and peptide receptor radionuclide therapy (PRRT, *e.g.* [^{90}Y]Y-DOTATATE). The lack of gamma ray or positron emission makes the detection of this radionuclide challenging. It is admittedly possible to perform biodistribution, imaging, and dosimetry studies using its Bremsstrahlung X-rays, though the poor resolution and quality of planar scintigraphic images and the requisite scintillation counting make these processes cumbersome [12]. Interestingly, it has been shown that the positrons emitted from yttrium-90 in very, very low abundance (0.003%) can yield positron emission tomography (PET) images with higher accuracy than Bremsstrahlung imaging, although this is not a routine—or clinically feasible—practice [12]. Ultimately, this lack of facile imaging means that a "matched nuclide pair" surrogate must be used to perform pre-therapy "scout" imaging to enable dosimetric measurements (see the sections on "Yttrium-86" and "Theranostics") [13–15].

One benefit to yttrium-90 compared to other therapeutic radionuclides is that it emits β^- particles with high energy ($E_{\beta^-(max)}$ = 2280 keV; see Table 1). The relatively long mean free path length of these β^- (~12 mm) means that they can be used to treat relatively large and poorly vascularized tumors [9, 16, 17]. Via this "crossfire effect," tumor cells up to ~550 cell diameters away from the radiopharmaceutical can receive therapeutic irradiation [9, 16]. This long β^- range is a double-edged sword, however, as it can lead to heightened damage to healthy tissues such as bone marrow (myelotoxicity) during the circulation of the radiopharmaceutical [18].

Yttrium-86

The positron-emitting radionuclide [^{86}Y]Y^{3+} ($t_{1/2}$ = 14.7 h, β^+ = 33%, $E_{\beta^+(mean)}$ = 535 keV average) can be produced with a cyclotron via the ^{86}Sr(p,n)^{86}Y reaction and can be purified by ion-exchange chromatography or electrolysis. However, this production route is notoriously difficult, and chemically pure yttrium-86 is difficult to obtain, as solutions of the radiometal often contain high concentrations of salts and other metal ion contaminants [19, 20]. Yttrium-86 is typically used for positron emission tomography (PET) by coupling it to targeting vectors such as peptides, antibodies, antibody fragments, and nanoparticles. Yttrium-86 is not used for radionuclide therapy, but its isotopolog yttrium-90 ejects high-energy β^- particles (electrons) and is often used for radionuclide therapy. Due to their chemical equivalence, a cancer-targeting molecule can be radiolabeled with yttrium-86 and used in cancer patients for pre-therapy PET scans to select patients with high tumor uptake and perform dosimetry. Depending on the outcome of the pre-therapy PET scan (scouting scan), the same molecule can then be radiolabeled with yttrium-90 and administered to the same patients for cancer therapy due to the cell-killing abilities of the high-energy β^- particles.

It is often useful to contrast the nuclear properties of exotic positron-emitting nuclides such as yttrium-86 with those of the "gold standard" radionuclide for PET: fluorine-18. Fluorine-18 has a very high positron abundance (96% of decay events result in a positron) and a low average β^+ energy of 252 keV [21, 22]. Yttrium-86, in contrast, has a low branching ratio of ~33%, emits 102 different gamma rays with energies ranging from 139 to 4900 keV (25% of which are within PET detection window of 350–650 keV), and ejects positrons with a significantly higher average energy of 535 keV [10, 23, 24]. This has practical significance for PET imaging. Upon the decay of a radionuclide, the ejected positron travels a distance that is dependent upon its kinetic energy. The ejected positron must lose all of its kinetic energy (net linear momentum = 0) before meeting an electron and annihilating into two 511 keV gamma rays. Positrons that are ejected with higher energy will travel further in the body before coming to rest and annihilating into detectable gamma rays. Consequently, positrons with higher energy produce PET images with lower spatial resolution [24].

The relationship between positron energy and image resolution is illustrated in Fig. 1, which depicts a common device

used for calibrating PET scanners called a phantom. These phantoms are filled with a homogenous aqueous solution containing the radionuclide of interest and three different sealed rods containing water, air, or Teflon. These three different sealed rods have different attenuation coefficients, which are values that describe the degree to which photons are absorbed or scattered by each medium (Teflon > water > air). These phantom images help to predict the spatial resolution that a specific positron-emitting radionuclide will have in animals and humans. In this figure, PET images of phantoms filled with homogenous aqueous solutions of fluorine-18, iodine-124, or yttrium-86 are shown to demonstrate the inferior spatial resolution of yttrium-86 (though modern software background correction can improve this somewhat) [25]. Yttrium-86 is especially poor at detecting bone lesions, as bone has a high attenuation coefficient, which together with the large number of gamma coincidences from yttrium-86 introduces a lot of error and noise. This is demonstrated dramatically by the Teflon rod (see Fig. 1, top rod), as Teflon has a similar attenuation coefficient to bone [26].

Other positron-emitting radiometals could be used for dosimetry scans prior to yttrium-90 therapy, including copper-64 ($E_{\beta^+(\text{mean})}$ = 278 keV, $R_{\beta^+(\text{mean})}$ = 0.7 mm) and zirconium-89 ($E_{\beta^+(\text{mean})}$ = 396 keV, $R_{\beta^+(\text{mean})}$ = 1.3 mm). However, neither of these radiometals are well matched to $[^{90}Y]Y^{3+}$ in terms of coordination chemistry or radionuclidic half-life [27]. A more detailed comparison of $[^{64}Cu]Cu^{2+}$ and $[^{90}Y]Y^{3+}$ highlights these problems. In addition to vastly different half-lives ($t_{1/2}$ = ~13 h for copper-64, $t_{1/2}$ = ~64 h for yttrium-90), the complexes of $[^{90}Y][Y(DOTA)]^{1-}$ compared with $[^{64}Cu][Cu(DOTA)]^{2-}$ have different coordination numbers (CN = 8, 6, respectively) and net charges, which result in significant discrepancies in their tumoral uptake and organ distribution [5]. Yttrium-86 effectively has the same half-life as copper-64 and therefore is a poor match with yttrium-90. However, the coordination chemistry and chemical properties of yttrium-86 are (of course) identical. As an aside, it is important to note that there are many discrepancies in nuclear decay properties reported in the literature, and so the values cited in this chapter should be considered approximate [9].

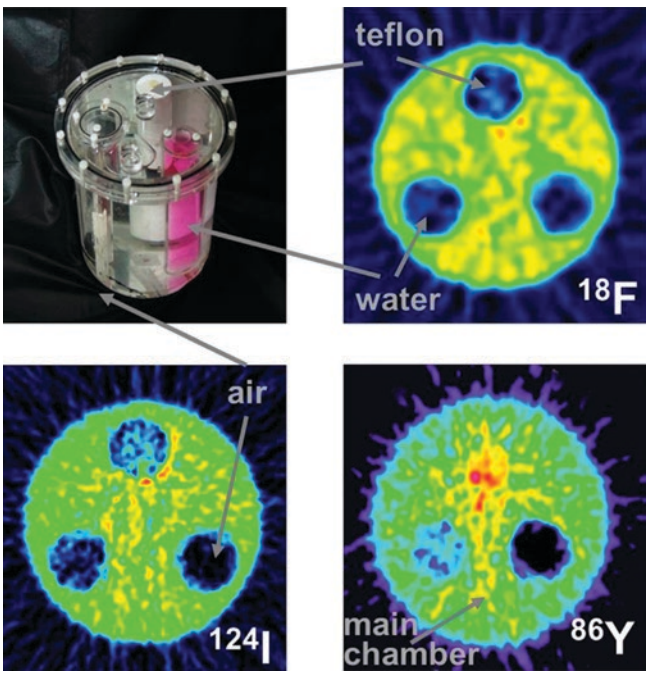

Fig. 1 Positron emission tomography (PET) images of three-rod (air, water, Teflon) phantoms showing the spatial resolution of select PET nuclides with no background subtraction of gamma coincidences (From Rösch *et al.* [26], with permission)

Lutetium-177

Lutetium-177 has a half-life of ~6.6 days and emits both β^- particles for therapy ($E_{\beta^-(\text{max})}$ = 497 keV) and gamma rays for single photon emission computed tomography (SPECT) imaging. As a result, lutetium-177 can be considered a true theranostic radionuclide [28, 29]. In practice, this means that SPECT imaging can be used to help evaluate the *in vivo* biodistribution of ^{177}Lu-labeled radiotherapeutics in the clinic. This approach does have two caveats. First, unlike PET, SPECT is not natively quantitative. And second, only a low abundance of the gamma rays emitted by lutetium-177 lies in the common SPECT imaging window (~30–300 keV), making long imaging times necessary and rendering imaging somewhat cumbersome. In addition to enabling theranostic applications, the gamma ray emissions from lutetium-177 also make biodistribution studies in animals and other *ex vivo* assays much easier. An additional difference between lutetium-177 and yttrium-90 is the energy of the β^- particles ejected from lutetium-177. The β^- particles emitted by lutetium-177 have a mean free path of ~1.6 mm in tissue, almost an order of magnitude shorter than those emitted by yttrium-90 (~12 mm). This shift results in not only lower myelotoxicity from lutetium-177 but also less tumorigenicity from the crossfire effect [18]. Differences in myelotoxicity may be substantial when attaching lutetium-177 and yttrium-90 to traditional peptide and antibody vectors that circulate in the blood for substantial periods of time. While these differences in physical properties may be significant, they *can* be circumvented using cutting-edge techniques in the design and administration of radiopharmaceuticals. Specifically, a recent study utilizing a pretargeted delivery approach vitro assays such as serum has shown improved dosimetry profiles and minimized these differences [30].

Although indium-111 ($t_{1/2}$ = ~67 h, gamma, SPECT) is commonly used for pre-therapy imaging for yttrium-90 and lutetium-177, SPECT imaging is generally inferior to PET. In Fig. 2 the same patient is imaged via SPECT with $[^{111}In]$In-DTPA-octreotide (4 h, 24 h) and via PET with $[^{86}Y]$Y-DOTATOC (4 h, 24 h), showing hepatic and para-aortic metastases of a carcinoid tumor [31]. This figure demonstrates that even though yttrium-86

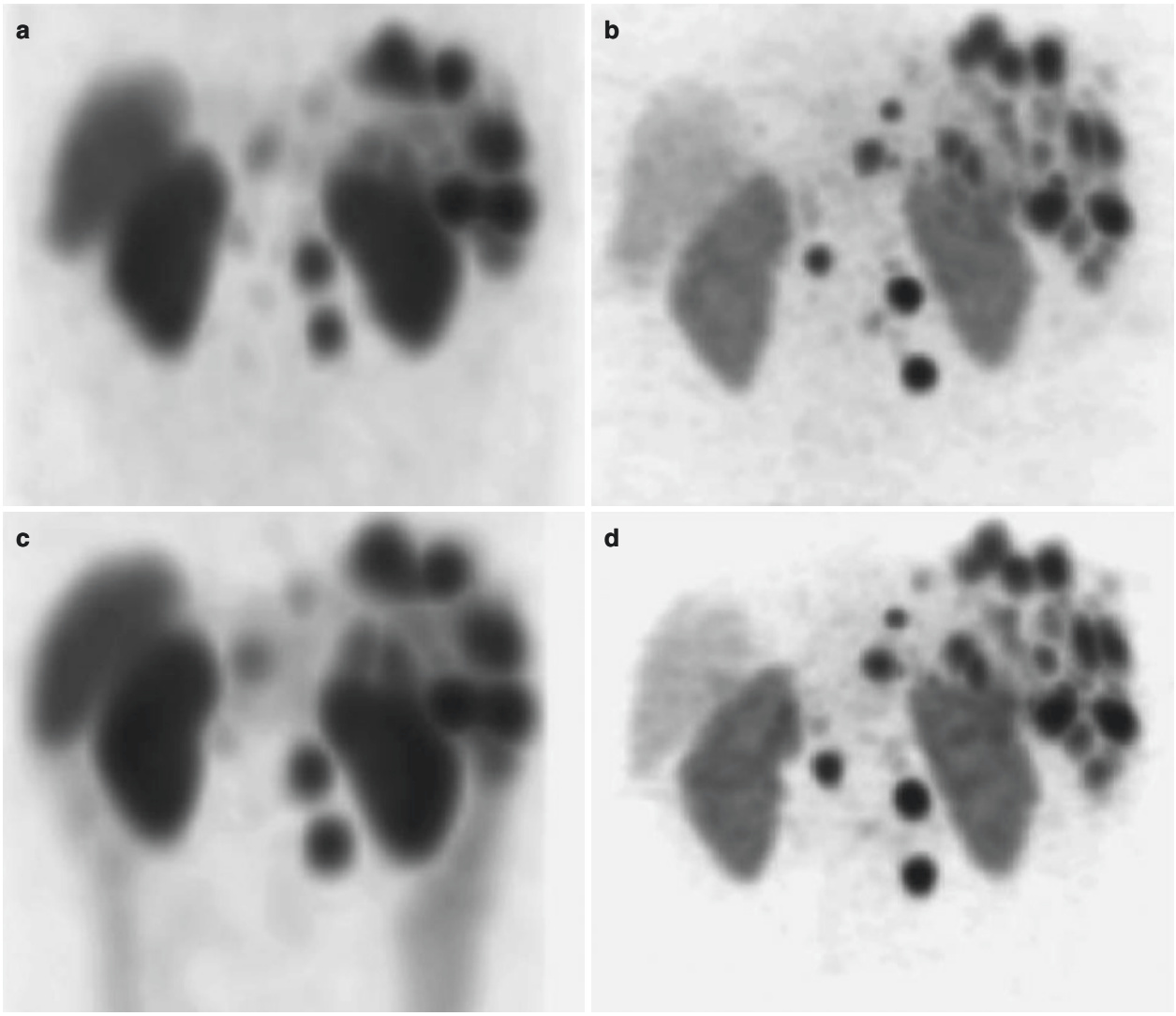

Fig. 2 The same patient imaged via single photon emission computed tomography (SPECT) with [^{111}In]In-DTPA-octreotide (4 h, 24 h, **a, c**) and via positron emission tomography (PET) with [^{86}Y]Y-DOTATOC (4 h, 24 h, **b, d**), showing hepatic and para-aortic metastases of a carcinoid tumor (From Förster *et al.* [31], with permission)

is one of the less desirable PET radionuclides due to its suboptimal nuclear decay properties, the resulting imaging quality is still superior to indium-111 SPECT.

Details

The Bioinorganic Chemistry of Lu^{3+} and Y^{3+}

Bioinorganic chemistry is the study of metals in biology, including the homeostasis and distribution of metals in the human body. Radiopharmaceuticals are administered in minuscule quantities, and so the metal-chelator coordination equilibrium has a strong driving force for dissociation. This is a fundamental reason why chelators must be very carefully tailored for each individual radiometal ion (*vide infra*), as the stability *in vivo* (kinetic inertness) of the metal-chelator complex must be remarkably high to ensure that the radiometal remains bound by the chelator. Within the body, several native ligands—including transferrin, serum albumin, ceruloplasmin, metallothioneins, phosphate, water, and halides—compete for the binding of the radiometal. Indeed, many of these native ligands exist at far higher concentrations than the chelator itself. The body maintains exquisite control and homeostasis of metal ions, and there are essentially no "free" metal ions in the body. Any radiometal that is released from a chelator will be quickly bound by serum proteins and shuttled through the blood either for storage, incorporation or adsorption into bone, binding by proteins/enzymes (*e.g.* superoxide dismutase/ceruloplasmin), or excretion.

To provide an example of metal regulation pertaining to radiometals, the metal ion Fe^{3+} is bound with very high

affinity by the blood serum protein transferrin (a native iron transport protein). However, larger cationic metal ions such as Y^{3+} and Lu^{3+} are not bound as tightly [32–35]. The metal ions Y^{3+} and Lu^{3+} have been shown to bind to transferrin, albeit not as strongly and more transiently than Fe^{3+} [32–35]. An obvious hypothesis for the weaker binding of the lanthanides to transferrin would be their size being too large to fit into the binding sites, as they have smaller charge-to-radius ratios and utilize 4f orbitals, resulting in lower metal ion binding affinity, as 4f orbitals are more diffuse than 3d orbitals [33]. It has been suggested that large metal ions bind poorly to transferrin largely due to steric repulsion at the more crowded *C*-terminus binding site [34], but a more sophisticated argument suggests that the binding strength of metal ions to transferrin is better related to metal ion acidity than size [36–38]. This hypothesis is supported by evaluating the large and very acidic metal ion Bi^{3+}, which has an abnormally high binding affinity for transferrin despite its size, which provides credence to this idea (103 pm, log K_1 = 19.4, and log K_2 = 18.5) [36–38]. Both arguments predict low binding affinities for Y^{3+} and Lu^{3+} for transferrin. The stability constants for binding transferrin with Y^{3+} have not been determined to our knowledge, but log K_1* = 11.08 and log K_2* = 7.93 have been reported for one or two Lu^{3+} ions, which are several orders of magnitude lower than the corresponding values for Fe^{3+} ions [34].

The radionuclides of yttrium and lutetium *do* have high affinity for bone, and the *in vivo* presence of "free" unchelated metal ions results in high uptake in bone. For example, ~50% of $[^{90}Y]Y^{3+}$ injected as unchelated metal ion into a human will primarily deposit in bone, with the next highest uptake being in the liver (~25%) [39]. More concerning is a study that suggests that even intact, cationic lanthanide complexes can adsorb onto the surface of bone. This means that even stably chelated radiometals may accumulate in the bone under certain circumstances, although this is less likely when the chelator is attached to a targeting vector such as an antibody or a peptide [40]. The take-home message from this evaluation of bioinorganic chemistry in relation to $[^{177}Lu]Lu^{3+}$ and $[^{86}Y]/[^{90}Y]Y^{3+}$ is that bone and liver uptake are two of the largest concerns, and abnormally high uptake of radiometal ions in these organs may indicate instability in the metal-chelator complex.

Bifunctional Chelators for Lu^{3+} and Y^{3+}

Chelators generally come in two broad types, macrocyclic and acyclic. Macrocycles are rigid and contain a partially preorganized binding site for the metal ion. The macrocycle effect—an extension of the chelate effect—leads to macrocyclic ligands generally forming more kinetically inert and thermodynamically stable complexes than comparable acyclic chelators [41]. Like the chelate effect, the macrocycle effect is primarily entropy-driven (thermodynamic): the preorganization of the chelator's binding groups means that less reorganization is required to wrap around a metal ion than is typically needed with acyclic chelators [41]. Practically speaking, this means that higher temperatures (*e.g.* 50–95 °C) are typically required to overcome this energetic barrier during radiolabeling reactions with macrocyclic chelators. On the flip side, however, macrocycles also possess high-energy barriers to the release of metal ions, a trait which results in excellent *in vivo* stability (kinetic inertness).

Acyclic chelators are linear (*i.e.* are not covalently cyclized) and are typically radiolabeled efficiently at ambient temperatures in as little as 5–15 min. This ease of radiolabeling portends the fact that acyclic chelators have lower energetic barriers to dissociation and are typically less stable than macrocycles *in vivo* (lower kinetic inertness). Thermodynamic stability constants (K_{ML} = [ML]/[M][L]) can be calculated from experiments such as potentiometric and/or spectrophotometric titrations, but these values offer practically zero predictive power when it comes to *in vivo* stability [42, 43]. Stability constants give a value, direction, and magnitude of the equilibrium in a metal-chelator coordination reaction, but they contain no kinetic information. The "kinetic inertness" of radiometal complexes is generally not quantifiable in terms of formal rate constants but rather tested indirectly via *in vitro* assays such as serum stability or by monitoring *in vivo* demetallation indirectly from characteristics such as bone uptake or liver uptake. Given the luxury, one would always opt for maximum stability and therefore choose macrocyclic chelators. However, sometimes fast radiolabeling kinetics are required (*e.g.* when using a short-lived nuclide), or high temperatures must be avoided (*e.g.* when using heat-sensitive biomolecules). In these cases, acyclic chelators are preferred or sometimes necessary.

A final consideration is that a chelator must be constructed to contain a reactive moiety that enables its facile conjugation to targeting vectors. A selection of these groups includes *N*-hydroxysuccinimidyl esters for the formation of peptide bonds, benzyl isothiocyanates for the formation of thiourea linkages, azides and alkynes for copper-catalyzed click chemistry, thiols and maleimides for the formation of thioether bonds, and tetrazines and *trans*-cyclooctenes for copper-free click chemistry. In the end, the most important experiments to determine the effective stability of both the chelator-radiometal complex and the bioconjugation method are *in vivo* biodistribution and imaging studies with direct comparisons to alternative chelators.

The two most successful and commonly used chelators for yttrium and lutetium are DOTA and CHX-A″-DTPA, but other new chelators such as the picolinic acid-based H_4octapa and the NOTA-based 5p-*C*-NETA have shown promise as well (Fig. 3)

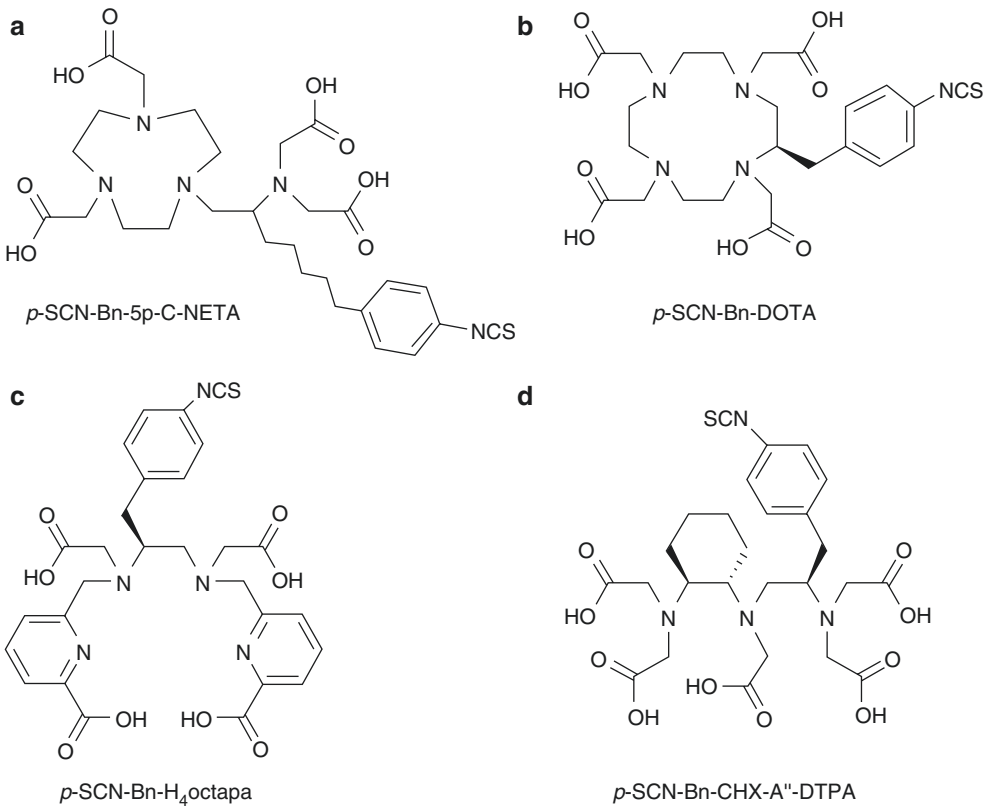

Fig. 3 The most popular and commercially available bifunctional derivatives of the chelators (**a**) 5p-*C*-NETA and (**b**) DOTA (**c**) H_4octapa and (**d**) CHX-A″-DTPA used for radiolabeling with $[^{177}Lu]Lu^{3+}$ and $[^{86}Y]/[^{90}Y]Y^{3+}$

[5, 44–51]. Commercial availability is a huge factor in adoption of chelators, and the front-runners [(*R*)-2-amino-3-(4-isothiocyanatophenyl)propyl]-trans-(*S,S*)-cyclohexane-1,2-diamine-pentaacetic acid (*p*-SCN-Bn-CHX-A″-DTPA) and S-2-(4-Isothiocyanatobenzyl)-1,4,7,10-tetraazacyclododecane tetraacetic acid (*p*-SCN-Bn-DOTA) can be purchased. Despite its slow radiolabeling kinetics and requisite high-temperature labeling conditions, DOTA is perhaps the most ubiquitous chelator used for radiometallation reactions. DOTA is generally considered the "gold standard" chelator for radiometal ions such as $[^{111}In]In^{3+}$, $[^{177}Lu]Lu^{3+}$, $[^{86}Y]/[^{90}Y]Y^{3+}$, $[^{225}Ac]$, $[^{44}Sc]/[^{47}Sc]Sc^{3+}$, and even $[^{68}Ga]Ga^{3+}$.

Particularly Important Works

Chelator Development: The Story of CHX-A″-DTPA

DTPA is the prototypical acyclic chelator for radiochemistry, and although it can bind many radiometal ions quickly at ambient temperature (< 30 min), universally poor *in vivo* stability and the emergence of CHX-A″-DTPA have made it obsolete [42]. The inadequacies of DTPA have been improved through the design of novel derivatives. The first successful alternative to DTPA was 1B4M-DTPA (tiuxetan), a ligand that only differs from DTPA in a single methyl group on one of its ethylene backbones. 1B4M-DTPA was used in the FDA-approved ^{90}Y-based drug Zevalin (Fig. 4) [52]. A further enhancement of DTPA came with CHX-A″-DTPA, in which the placement of a cyclohexyl moiety in the chelator backbone made the chelator more rigid compared to native DTPA. In essence, the inclusion of this cyclohexyl group imposes a degree of covalent preorganization, making CHX-A″-DTPA a "pseudo-macrocycle." The enhanced *in vivo* stability (kinetic inertness) gained from these changes came at the expense of radiolabeling kinetics. That said, the radiolabeling of CHX-A″-DTPA is still very efficient between 20 °C and 37 °C and much more reliable and reproducible than DOTA [42, 53].

In principle, the metal-chelator portion of a radiometal-based radiopharmaceutical should have no influence on the ability of the vector to engage its target (*e.g.* receptor), assuming that there is sufficient space between the chelator and the target-binding portion of the vector. Following this logic, the stereochemistry of a chelator should not affect the *in vivo* behavior of a biomolecular vector, as the chelator itself is not binding to the receptor. However, it is possible that the stereochemistry of the chelator *could* impact the *in vivo* behavior of a radiopharmaceutical by influencing the coordination chemistry, geometry, charge, or stability of the chelator-radiometal complex. In this regard, the family of cyclohexyl-modified DTPA chelators are particularly interesting. Indeed, there are four stereoisomers of

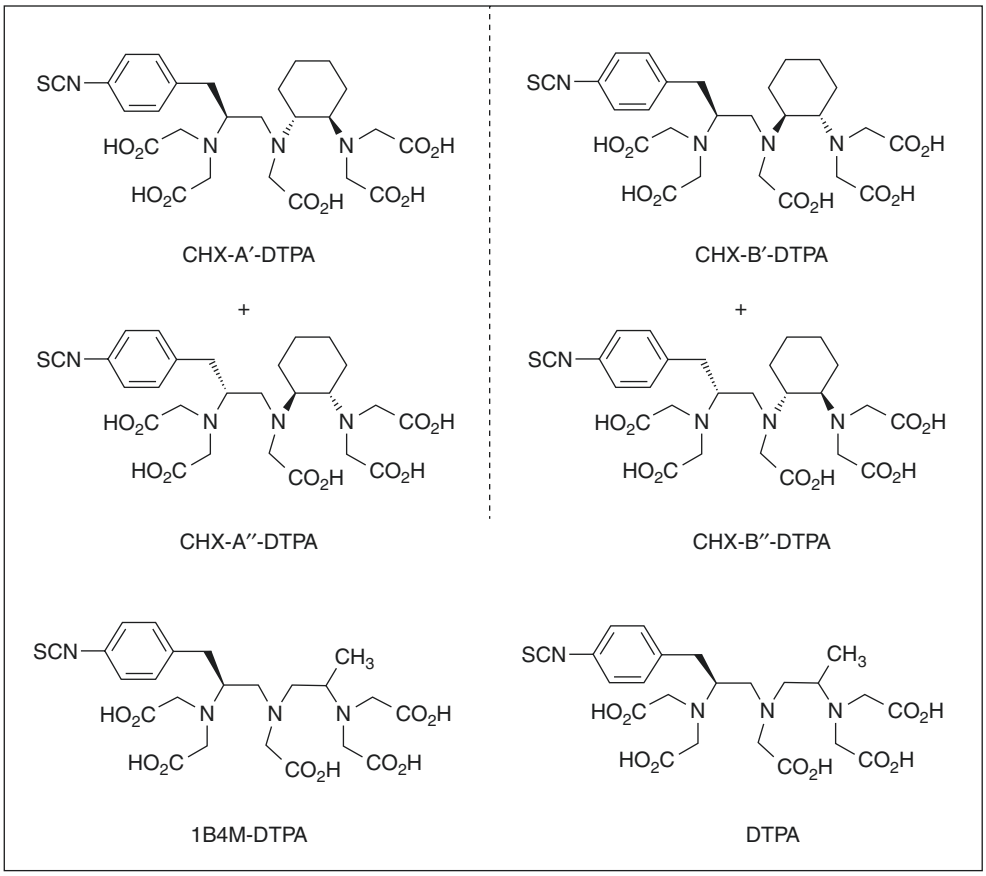

Fig. 4 Chemical structures of the four isomers of CHX-DTPA as well as the chelators 1B4M-DTPA and DTPA, depicted in their bifunctional benzyl isothiocyanate forms

cyclohexyl-modified DTPA: CHX-A′-DTPA, CHX-A″-DTPA, CHX-B′-DTPA, and CHX-B″-DTPA (see Fig. 4). Remarkably, Brechbiel and coworkers went to the trouble of synthesizing each isomer, radiolabeling it with [^{90}Y]Y^{3+}, and assaying its *in vivo* behavior [51]. A critical concept emerged from this study: the [^{90}Y]Y-CHX-B″-DTPA isomer was substantially less stable *in vivo* than the [^{90}Y]Y-CHX-A″-DTPA isomer, as demonstrated by the activity concentrations in the bone (~12 %ID/g vs ~4 %ID/g, respectively) [42, 51]. As previously discussed, when released *in vivo*, unchelated yttrium and lutetium primarily end up adsorbing or otherwise incorporating into bone. This fact allows bone uptake values to be used as surrogate markers for the stability of their radiometal complexes *in vivo*. To our knowledge, the exact reason for this difference in stability between isomers has not been elucidated; however, it is likely that the covalent preorganization imposed by the less stable isomers of CHX-DTPA forces inferior overlap between the orbitals of the metal and ligand. This result highlights the importance of the enantiopurity of chelators in cases in which stereochemistry can impact the coordination of the radiometal. Clearly, the use of a racemic mixture of CHX-DTPA variants would result in higher background uptake of [^{90}Y]Y^{3+} than the use of enantiomerically pure [^{90}Y]Y-CHX-A″-DTPA [42, 51].

Theranostics

Perhaps the most common application of yttrium-86 is as a theranostic pair nuclide for yttrium-90. The term "theranostic" typically refers to the use of the same chemical agent (*e.g.* a chelator-antibody conjugate) for both diagnostic and therapeutic applications in personalized medicine. In some cases, the different emissions from a single radionuclide (*e.g.* lutetium-177) can be harnessed for both imaging and therapy. In other cases, this is not possible, and two different versions of the same radiopharmaceuticals must be employed: one labeled with a nuclide for imaging and one labeled with a nuclide for therapy.

Given that radionuclides that emit both photons for imaging as well as particles for therapy are somewhat rare, the latter approach is more common. In this regard, one can imagine using a chelator-antibody conjugate labeled with a positron-emitting nuclide for PET imaging and dosimetry calculations and then subsequently using the same chelator-antibody conjugate labeled with a β^--emitting nuclide for radioimmunotherapy at a later date. Ideally, a "matched nuclide pair" with nearly identical chemical and nuclear decay characteristics would be used. Unfortunately, these pairs are difficult to find. One common pairing is indium-111 ($t_{1/2}$ = ~67 h, gamma, SPECT) and yttrium-90 ($t_{1/2}$ = ~64 h,

β⁻, therapy). However, this pairing is not ideal due to differences in the coordination spheres and nuclear properties of [^{111}In]In^{3+} and [^{90}Y]Y^{3+}.

It is perhaps not surprising that using yttrium-86 as a theranostic pair nuclide for yttrium-90 has received a great deal of attention. The primary benefit of this pairing is the chemical indistinguishability of [^{86}Y]Y^{3+} and [^{90}Y]Y^{3+}. As a result, radiopharmaceuticals labeled with these two radionuclides of yttrium are biologically equivalent surrogates, making ^{86}Y-labeled constructs ideal for imaging scans used to predict the biodistribution and dosimetry of ^{90}Y-labeled therapeutics. The primary drawback of this theranostic pair is that the half-life of yttrium-86 (14.7 h) is significantly shorter than that of yttrium-90 (64.2 h). As a result, PET data beyond 1–3 days post injection is not available with yttrium-86, though this information could be important when considering the *in vivo* performance of ^{90}Y-labeled radiopharmaceuticals [14, 15]. Despite this limitation of ^{86}Y-PET, PET is generally preferred to SPECT because the former provides improved spatial resolution, produces quantitative data, is natively 3D, and has greater sensitivity, thus enabling more rapid scans with lower injected doses [12].

Several examples of the use of ^{86}Y- and ^{90}Y-labeled theranostic pairs have been published. In one, the authors found that [^{86}Y]Y-CHX-A″-DTPA-trastuzumab provided superior images and more accurate dosimetry data compared to [^{111}In]In-CHX-A″-DTPA-trastuzumab as an imaging surrogate for radioimmunotherapy with [^{90}Y]Y-CHX-A″-DTPA-trastuzumab [14]. Another study compared the accuracy of peptide receptor radionuclide therapy (PRRT) dosimetry performed with [^{86}Y]/[^{111}In]Y/In-DOTATOC for scouting scans prior to [^{90}Y]Y-DOTATOC therapy [31, 54]. This study revealed that [^{111}In]In-DTPA-octreotide and [^{111}In]In-DOTATOC were not biologically equivalent to the ^{90}Y-/^{86}Y-labeled analogues and yielded different organ distributions and inaccurate dosimetry data [31, 54]. These studies demonstrate the well-established principle that performing pre-therapy scouting scans with a chemically identical radiometal surrogate (theranostics) such as yttrium-86 for yttrium-90 is not *required* but is *ideal* when appropriate radionuclides are accessible [14, 31, 54]. The current gold standard in theranostic medicine can be found in the domain of PRRT, where [^{68}Ga]Ga-DOTATATE and other somatostatin-targeting peptide derivatives are used for PET imaging diagnosis and dosimetry, followed by [^{177}Lu]- or [^{90}Y]-DOTATATE therapy (and more recently actinium-225). In fact, [^{177}Lu]Lu-DOTATATE was FDA approved in January 2018 under the brand name LUTATHERA®. A recent clinical study has demonstrated success using tandem PRRT for treating neuroendocrine tumors, which utilized co-injection of both [^{90}Y]Y- and [^{177}Lu]Lu-DOTATATE [55]. The success of this study was reliant on the use of [^{68}Ga]Ga-DOTATATE PET for pre-therapy dosimetry, as well as post-therapy monitoring of treatment response [55].

Tricks of the Trade: Moles and Specific Activity

A thought exercise on specific activity is often useful to put the quantities of a radionuclide used during radiolabeling reactions in perspective and place concrete values on frequently used terms such as "sub-pharmacological." On the information sheets for its products, one of the major radionuclide distributors in North America lists specific activities of 740 GBq/mg for lutetium-177 and 18,500 GBq/mg for yttrium-90. For a research radiolabeling experiment, quantities of 1–20 mCi (37–740 MBq) may typically be used. As summarized in Table 2, a 10 mCi (370 MBq) aliquot of lutetium-177 at a specific activity of 20 Ci/mg (3538 Ci/mmol) is a physical quantity of only ~500 ng and ~2.8 nmol. For yttrium-90, 10 mCi (370 MBq) at a specific activity of 500 Ci/mg (44,954 Ci/mmol) corresponds to a physical quantity of ~20 ng, which is only ~0.2 nmol. To put this in perspective, a standard bottle of concentrated HCl contains ~0.2 ppm iron. It's common to add ~10 μL of concentrated HCl while adjusting the pH of a radiometal solution or buffer, which means adding ~0.036 nmol of Fe^{3+}. To put this into context, a radiolabeling reaction containing 1 mCi (37 MBq) of [^{90}Y]Y^{3+} is only ~0.02 nmol, which means that adding 10 μL of concentrated HCl will introduce a molar excess of iron (~0.036 nmol). This highlights the reason why expensive metal-free acids are typically used for adjusting the pH of radiolabeling buffers (they contain ppb levels of iron instead of ppm), and a metal-scavenging resin such as Chelex® 100 is often used to pretreat buffers. For this thought experiment, we will consider the real-world example of radiolabeling the chelator-bearing immunoconjugate DOTA-trastuzumab. DOTA is a chelator typically used for coordinating [^{90}Y]Y^{3+} and [^{177}Lu]Lu^{3+}, and trastuzumab is a commonly used monoclonal antibody that targets the HER2/*neu* receptor which is overexpressed by a variety of human tumors. In most cases a 1:1 stoichiometric ratio of chelator/radiometal is not achievable when preparing radiopharmaceuticals, as this would mean literally every single molecule of the chelator-antibody conjugate had bound a radiometal ion. Although not realistically achievable, these calculated values effectively provide a value for the "theoretical 100% yield," which would provide the maximum possible specific activity (Max SA; see Table 2).

Tricks of the Trade: Radiolabeling Tips

General radiolabeling protocols for [^{177}Lu]Lu^{3+}, [^{90}Y]Y^{3+}, and [^{86}Y]Y^{3+} dictate that once a solution of radiometal ion is procured (usually as an acidic solution in 0.05–0.1 M HCl or nitric acid), the desired quantity of activity is transferred via auto-pipette to a chelator-vector bioconjugate in buffer. This radiolabeling mixture is allowed to react until radiolabeling yields are as high as possible given the chosen chelator, concentration, and temperature conditions [14, 42, 56, 57]. Radiolabeling yields are typically determined via radioactive instant thin-layer chromatography (called "iTLC") or reverse-phase HPLC coupled to a radiation detector. The chelation of radiometal ions typically requires 15–120 min, depending on the chelator and reaction temperature used. After radiolabeling, the aqueous reaction mixture is purified before use. When the targeting vector is an antibody or large protein, purification is typically performed via size-exclusion chromatography with an appropriate molecular weight cut-off (*e.g.* PD10 Sephadex G25 columns or centrifuge spin filters). Radiometallated peptide conjugates are typically purified via reverse-phase HPLC or small C_{18} Sep-Pak cartridge trap/release. The final prepared doses are typically formulated in saline, are filtered through a 0.22 μm syringe filter for sterilization, and sometimes include a radioprotectant such as ascorbic acid or gentisic acid.

To unpack these variables in more detail, the factor of temperature relates to the type of chelator, with acyclic chelators such as CHX-A″-DTPA typically needing 15–60 min at room temperature or 37 °C to obtain good radiolabeling yields. Even when acyclic chelators are employed, they are sometimes heated to improve radiolabeling efficiency with certain vectors. On the other hand, macrocyclic chelators such as DOTA exhibit slow radiolabeling kinetics and require temperatures in the range of 70–100 °C for 15–60 min for effective and reproducible labeling. To the detriment of reproducibility and radiochemical yields, DOTA-bearing antibodies are routinely radiolabeled at only 37 °C due to the temperature sensitivity of large proteins. The caveats to radiolabeling DOTA at 37 °C are the low and—even more

Table 2 Thought exercise demonstrating common mass and mole quantities of radiometal nuclides used for radiolabeling trastuzumab (10 mCi = 370 MBq). The calculation assumes only one chelator per antibody (146 kDa, 1:1 molar ratio of radiometal/antibody); SA = specific activity

Nuclide	SA (Ci/mg)	SA (Ci/mmol)	Mass of 10 mCi nuclide (ng)	Moles of 10 mCi nuclide (nmol)	Max SA for 1 mg trastuzumab labeling (mCi/mg)
[^{177}Lu]Lu^{3+}	20	3538	500	2.8	24.2
[^{90}Y]Y^{3+}	500	44,954	20	0.2	308

Sample calculations for lutetium-177 →

$$\text{SA of } [^{177}\text{Lu}]\text{Lu}^{3+} = \left[20\frac{\text{Ci}}{\text{mg}}\times 10^{3}\frac{\text{mg}}{\text{g}}\times 176.904\frac{\text{g}}{\text{mol}}\times 10^{-3}\frac{\text{mol}}{\text{mmol}}\right] = 3538\frac{\text{Ci}}{\text{mmol}}$$

$$\text{Mass of 10 mCi of } [^{177}\text{Lu}]\text{Lu}^{3+} = \left[10\,\text{mCi}\times 10^{-3}\frac{\text{Ci}}{\text{mCi}}\times\frac{1\,\text{mg}}{20\,\text{Ci}}\times 10^{6}\frac{\text{ng}}{\text{mg}}\right] = 500\,\text{ng}$$

$$\text{Moles of 10 mCi of } [^{177}\text{Lu}]\text{Lu}^{3+} = \left[10\,\text{mCi}\times 10^{-3}\frac{\text{Ci}}{\text{mCi}}\times\frac{1\,\text{mmol}}{3538\,\text{Ci}}\times 10^{6}\frac{\text{nmol}}{\text{mmol}}\right] = 2.8\,\text{nmol}$$

Maximum theoretical SA for 1 mg trastuzumab labeling →

$$\text{Moles of 1 mg trastuzumab} = \left[\frac{1\,\text{mg}\times 10^{-3}\frac{\text{g}}{\text{mg}}}{146{,}000\frac{\text{g}}{\text{mol}}}\times 10^{9}\frac{\text{nmol}}{\text{mol}}\right] = 6.85\,\text{nmol}$$

1:1 ratio → Moles of lutetium-177 = 6.85 nmol

$$\text{SA } [^{177}\text{Lu}]\text{Lu-trastuzumab} = \left[\left(6.85\times 10^{-6}\,\text{mmol}\right)\times 3538\frac{\text{Ci}}{\text{mmol}}\times 10^{3}\frac{\text{mCi}}{\text{Ci}}\right] = 24.2\frac{\text{mCi}}{\text{mg}}$$

problematically—inconsistent radiochemical yields. The most common buffers used with these radiometal ions are sodium or ammonium acetate at pH 4.5–5.5 (~0.2–2.0 mL, 200–1000 mM). The molarity of these buffers depends on the volume of the acidic solution of radiometal that is added. As radiometals are typically delivered as 0.05–0.1 M HCl solutions, buffers with higher molarities can be used to ensure that the addition of the solution of radiometal to small volumes of the buffer will not change the pH of the radiolabeling reaction. This allows the reaction volume to be kept as small as possible, which improves radiolabeling yields. As mentioned in the thought exercise on specific activity, buffers are typically prepared with trace-level metal-free chemicals and then treated with a metal-scavenging resin such as Chelex® 100 (~1.2 g/L Chelex® in prepared buffer, stirred overnight, and then filtered to remove spent resin) in order to remove as many contaminant metal ions as possible.

The radionuclides $[^{177}Lu]Lu^{3+}$ and $[^{90}Y]Y^{3+}$ emit ionizing β-particles, which causes water molecules to undergo radiolysis (bond cleavage generating free radicals). Free radicals created by the radiolysis of water, including hydroxyl radicals and superoxide radicals, can then destroy the radiopharmaceutical (vector). All radionuclides in high enough quantities and concentrations can induce solvent radiolysis and generate free radicals [58]. Consequently, when radiolabeling with large activities of either of these radionuclides, adding ~1–10 mg/mL (~5–50 mM) of ascorbic acid can act as a radioprotectant to minimize the damage to the radiotracer cause by free radicals [55]. Another consideration when radiolabeling with these radionuclides is that the *chemical purity* differs between radiometals and also between production locations. Excess quantities of non-radioactive contaminant metal ions can drastically interfere with radiolabeling yields, as the chelator may become saturated with other metal ions before it can coordinate the desired radiometal (this is often an issue with yttrium-86).

Controversial Issues: The Dark Side of Yttrium-86

Some shortcomings of yttrium-86 were listed above, such as the poor resolution of its PET images due to the high energy of its ejected positrons, the difficulty of its purification after production, its short half-life compared to its partner nuclide yttrium-90, and its emission of 105 different gamma rays. Some of these deficiencies can be overcome. For example, a software can be used to subtract some of the prompt gamma events after imaging and thus improve the quality of yttrium-86 PET images. Others, however, cannot. For example, the plethora of gamma rays emitted from yttrium-86 require significant shielding, resulting in transportation and logistical problems as well as a radiation dose concern for the personnel handling the radionuclide [9]. In addition, the difficulty in purifying yttrium-86 and the consequent low radiochemical yields obtained by using impure radiometal remain stubborn issues. Indeed, to the knowledge of this chapter's authors, a reliable commercial source of chemically pure yttrium-86 is not currently available in North America, although individual sites may produce it on an ad hoc basis. Taken together, these concerns force the inevitable conclusion that—at least for now—yttrium-86 is undeniably inferior to other positron-emitting nuclides such as fluorine-18, zirconium-89, and gallium-68 (see Figs. 1 and 2) [25, 59].

The Bottom Line

We hope this chapter has illuminated the various chemical and radiochemical properties of lutetium-177, yttrium-90, and yttrium-86 that have made them popular choices for nuclear imaging and therapy over the previous decades. Indeed, these three radionuclides are commonly used with peptide-, antibody-, and nanoparticle-based targeting vectors for SPECT, PET, and radionuclide therapy. Although yttrium-86 remains a troublesome and niche radiometal with very limited availability and many undesirable properties, lutetium-177 and yttrium-90 are two of the most commonly used therapeutic radionuclides worldwide.

- Lutetium-177 ($[^{177}Lu]Lu^{3+}$, $t_{1/2}$ = ~159 h, $E_{\beta^-(max)}$ = 497 keV, $R_{\beta^-(mean)}$ = 1.6 mm, γ = 112, 208 keV):
  - Emits β-particles for radiotherapy as well as gamma rays for SPECT imaging, therefore making it a theranostic radiometal.
  - Emits gamma rays with low abundance. This combined with the low sensitivity of SPECT makes imaging with this radionuclide sub-optimal.
  - Is typically utilized with the chelators DOTA or CHX-A″-DTPA.
  - Is mostly used with peptide- or antibody-based targeting vectors.
  - Has radiochemistry and chelator selection that is effectively identical to that of yttrium-86/yttrium-90.
  - Emits β-particles with a short mean free path length of ~1.6 mm *in vivo*. This not only minimizes radiation toxicity but also reduces crossfire effect and therapeutic efficacy compared to yttrium-90.
  - Emits gamma rays upon decay, which make handling and analysis easier than yttrium-90.
  - Can be purchased with a specific activity of ~20–100 Ci/mg (~740–3700 GBq/mg), which is much lower than that of commercially available yttrium-90 at ~500 Ci/mg (18,500 GBq/mg).

- Yttrium-90 ($[^{90}Y]Y^{3+}$, $t_{1/2}$ = 64.1 h, $E_{\beta^-(max)}$ = 2280 keV, $R_{\beta^-(mean)}$ = 12 mm, 0.003% β^+):
  - Strictly emits high-energy electrons (β^-) for radiotherapy, and its decay produces no substantial quantity of gamma rays or positrons (β^+), making both handling and analysis difficult.
  - Emits β-particles with a longer mean free path length of ~12 mm *in vivo*, which not only increases radiation toxicity but also increases crossfire effect and therapeutic efficacy relative to lutetium-177.
  - Emits a very, very low abundance (0.003%) of positrons which have been imaged with PET. However, this is not trivial or performed routinely.
  - Requires that dosimetry must be performed using a different radionuclide, such as the yttrium-86, indium-111, gallium-68, or zironcium-89.
- Yttrium-86 ($[^{86}Y]Y^{3+}$, $t_{1/2}$ = 14.7 h, β^+ ratio = 33%, $E_{\beta^+(mean)}$ = 535 keV, $R_{\beta^+(mean)}$ = 2.5 mm):
  - Is chemically identical to yttrium-90 and therefore forms bioequivalent chelate complexes, yielding accurate dosimetry data from PET images.
  - Has a shorter half-life (14.7 h vs 64.1 h) that is a poor match for its isotopologue yttrium-90.
  - Produces PET images with relatively poor quality.
  - Emits 105 different gamma rays, which cause radiation shielding issues and dose concerns and require substantial lead shielding for handling and transport.
  - Lacks a reliable commercial source or a long-lived generator system, making the logistics of distribution and procurement challenging.
  - Has not seen much success or clinical interest, with investigators instead favoring gallium-68 or zirconium-89.

References

1. Pearson RG. Hard and soft acids and bases, HSAB, part I: fundamental principles. J Chem Educ. 1968;45(9):581.
2. Shannon R. Revised effective ionic radii and systematic studies of interatomic distances in halides and chalcogenides. Acta Crystallogr. 1976;A32(5):751–67.
3. Barnum DW. Hydrolysis of cations. Formation constants and standard free energies of formation of hydroxy complexes. Inorg Chem. 1983;22(16):2297–305.
4. Liu S. The role of coordination chemistry in the development of target-specific radiopharmaceuticals. Chem Soc Rev. 2004;33(7):445–61.
5. Price EW, Orvig C. Matching chelators to radiometals for radiopharmaceuticals. Chem Soc Rev. 2014;43(1):260–90.
6. Baes CF, Mesmer RE. The thermodynamics of cation hydrolysis. Am J Sci. 1981;281(7):935–62.
7. Baes CF Jr, Mesmer RE. The hydrolysis of cations. New York: Wiley-Interscience; 1976.
8. Martell AE, Smith RM. Critical stability constants. Vol. 3: other organic ligands. New York: Plenum Press; 1977.
9. Holland JP, Williamson MJ, Lewis JS. Unconventional nuclides for radiopharmaceuticals. Mol Imaging. 2010;9(1):1–20.
10. Walrand S, Jamar F, Mathieu I, De Camps J, Lonneux M, Sibomana M, et al. Quantitation in PET using isotopes emitting prompt single gammas: application to yttrium-86. Eur J Nucl Med Mol Imaging. 2003;30(3):354–61.
11. Lederer CM, Shirley VS. Table of isotopes. 7th ed. New York: Wiley; 1978.
12. Walrand S, Flux G, Konijnenberg M, Valkema R, Krenning E, Lhommel R, et al. Dosimetry of yttrium-labelled radiopharmaceuticals for internal therapy: 86Y or 90Y imaging? Eur J Nucl Med Mol Imaging. 2011;38(1):57–68.
13. Nayak TK, Garmestani K, Milenic DE, Baidoo KE, Brechbiel MW. HER1-targeted 86Y-panitumumab possesses superior targeting characteristics than 86Y-cetuximab for PET imaging of human malignant mesothelioma tumors xenografts. PLoS One. 2011;6(3):e18198.
14. Palm S, Enmon RM, Matei C, Kolbert KS, Xu S, Zanzonico PB, et al. Pharmacokinetics and biodistribution of 86Y-trastuzumab for 90Y dosimetry in an ovarian carcinoma model: correlative microPET and MRI. J Nucl Med. 2003;44(7):1148–55.
15. Herzog H, Rösch F, Stöcklin G, Lueders C, Qaim SM, Feinendegen LE. Measurement of pharmacokinetics of yttrium-86 radiopharmaceuticals with PET and radiation dose calculation of analogous yttrium-90 radiotherapeutics. J Nucl Med. 1993;34(12):2222–6.
16. Forrer F, Waldherr C, Maecke HR, Mueller-Brand J. Targeted radionuclide therapy with 90Y-DOTATOC in patients with neuroendocrine tumors. Anticancer Res. 2006;26(1B):703–7.
17. Volkert WA, Goeckeler WF, Ehrhardt GJ, Ketring AR. Therapeutic radionuclides: production and decay property considerations. J Nucl Med. 1991;32(1):174–85.
18. Baum RP, Kluge AW, Kulkarni H, Schorr-Neufing U, Niepsch K, Bitterlich N, et al. [(177)Lu-DOTA](0)-D-Phe(1)-Tyr(3)-octreotide ((177)Lu-DOTATOC) for peptide receptor radiotherapy in patients with advanced neuroendocrine tumours: a Phase-II study. Theranostics. 2016;6(4):501–10.
19. Sadeghi M, Aboudzadeh M, Zali A, Mirzaii M, Bolourinovin F. Radiochemical studies relevant to 86Y production via 86Sr(p,n)86Y for PET imaging. Appl Radiat Isot. 2009;67(1):7–10.
20. Reischl G, Rösch F, Machulla HJ. Electrochemical separation and purification of yttrium-86. Radiochim Acta. 2002;90(4):225–8.
21. Disselhorst JA, Brom M, Laverman P, Slump CH, Boerman OC, Oyen WJG, et al. Image-quality assessment for several positron emitters using the NEMA NU 4-2008 standards in the Siemens Inveon Small-Animal PET Scanner. J Nucl Med. 2010;51(4):610–7.
22. Jødal L, Loirec CL, Champion C. Positron range in PET imaging: an alternative approach for assessing and correcting the blurring. Phys Med Biol. 2012;57(12):3931.
23. Sadeghi M, Aboudzadeh M, Zali A, Zeinali B. 86Y production via 86Sr(p,n) for PET imaging at a cyclotron. Appl Radiat Isot. 2009;67(7):1392–6.
24. Jødal L, Loirec CL, Champion C. Positron range in PET imaging: non-conventional isotopes. Phys Med Biol. 2014;59(23):7419–34.
25. Lubberink M, Herzog H. Quantitative imaging of 124I and 86Y with PET. Eur J Nucl Med Mol Imaging. 2011;38(1):10–8.
26. Rösch F, Herzog H, Qaim S. The beginning and development of the theranostic approach in nuclear medicine, as exemplified by the radionuclide pair 86Y and 90Y. Pharmaceuticals. 2017;10(2):56.
27. Conti M, Eriksson L. Physics of pure and non-pure positron emitters for PET: a review and a discussion. EJNMMI Phys. 2016;3(1):8.
28. Dash A, Pillai MRA, Knapp FF. Production of (177)Lu for targeted radionuclide therapy: available options. Nucl Med Mol Imaging. 2015;49(2):85–107.

29. Baum RP, Kulkarni HR. Theranostics: from molecular imaging using Ga-68 labeled tracers and PET/CT to personalized radionuclide therapy – the Bad Berka experience. Theranostics. 2012;2(5):437–47.
30. Altai M, Membreno R, Cook B, Tolmachev V, Zeglis B. Pretargeted imaging and therapy. J Nucl Med. 2017;58(10):1553–9.
31. Förster GJ, Engelbach MJ, Brockmann JJ, Reber HJ, Buchholz HG, Mäcke HR, et al. Preliminary data on biodistribution and dosimetry for therapy planning of somatostatin receptor positive tumours: comparison of 86Y-DOTATOC and 111In-DTPA-octreotide. Eur J Nucl Med. 2001;28(12):1743–50.
32. Harris WR, Pecoraro VL. Thermodynamic binding constants for gallium transferrin. Biochemistry. 1983;22(2):292–9.
33. Harris WR, Chen Y. Difference ultraviolet spectroscopic studies on the binding of lanthanides to human serum transferrin. Inorg Chem. 1992;31(24):5001–6.
34. Harris WR, Yang B, Abdollahi S, Hamada Y. Steric restrictions on the binding of large metal ions to serum transferrin. J Inorg Biochem. 1999;76(3–4):231–42.
35. Harris WR. Binding and transport of nonferrous metals by serum transferrin. In: Clarke MJ, editor. Less common metals in proteins and nucleic acid probes. Structure and bonding, vol. 92. Berlin/Heidelberg: Springer; 1998. p. 121–62.
36. Sun H, Li H, Sadler PJ. Transferrin as a metal ion mediator. Chem Rev. 1999;99(9):2817–42.
37. Sun H, Cox M, Li H, Sadler P. Rationalisation of metal binding to transferrin: prediction of metal-protein stability constants. In: Hill H, Sadler P, Thomson A, editors. Metal sites in proteins and models. Structure and bonding, vol. 88. Berlin/Heidelberg: Springer; 1997. p. 71–102.
38. Li H, Sadler PJ, Sun H. Rationalization of the strength of metal binding to human serum transferrin. Eur J Biochem. 1996;242(2):387–93.
39. Ando A, Ando I, Hiraki T, Hisada K. Relation between the location of elements in the periodic table and various organ-uptake rates. Int J Rad Appl Instrum B. 1989;16(1):57–80.
40. Wang L, Shi J, Kim Y-S, Zhai S, Jia B, Zhao H, et al. Improving tumor-targeting capability and pharmacokinetics of 99mTc-labeled cyclic RGD dimers with PEG4 linkers. Mol Pharm. 2009;6(1):231–45.
41. Hancock RD. Chelate ring size and metal ion selection. The basis of selectivity for metal ions in open-chain ligands and macrocycles. J Chem Educ. 1992;69(8):615–21.
42. Camera L, Kinuya S, Garmestani K, Wu C, Brechbiel MW, Pai LH, et al. Evaluation of the serum stability and in vivo biodistribution of CHX-DTPA and other ligands for yttrium labeling of monoclonal antibodies. J Nucl Med. 1994;35(5):882–9.
43. Harrison A, Walker CA, Parker D, Jankowski KJ, Cox JPL, Craig AS, et al. The in vivo release of 90Y from cyclic and acyclic ligand-antibody conjugates. Int J Rad Appl Instrum B. 1991;18(5):469–76.
44. Price EW, Carnazza KE, Carlin SD, Cho A, Edwards KJ, Sevak KK, et al. 89Zr-DFO-AMG102 immuno-PET to determine local HGF protein levels in tumors for enhanced patient selection. J Nucl Med. 2017;58(9):1386–94.
45. Price EW, Edwards KJ, Carnazza KE, Carlin SD, Zeglis BM, Adam MJ, et al. A comparative evaluation of the chelators H4octapa and CHX-A″-DTPA with the therapeutic radiometal 90Y. Nucl Med Biol. 2016;43(9):566–76.
46. Price EW, Cawthray JF, Adam MJ, Orvig C. Modular syntheses of H4octapa and H2dedpa, and yttrium coordination chemistry relevant to 86Y/90Y radiopharmaceuticals. Dalton Trans. 2014;43(19):7176–90.
47. Price EW, Zeglis BM, Cawthray JF, Lewis JS, Adam MJ, Orvig C. What a difference a carbon makes: H4octapa vs. H4C3octapa, ligands for In-111 and Lu-177 radiochemistry. Inorg Chem. 2014;53(19):10412–31.
48. Price EW, Zeglis BM, Cawthray JF, Ramogida CF, Ramos N, Lewis JS, et al. H4octapa-trastuzumab: versatile acyclic chelate system for 111In and 177Lu imaging and therapy. J Am Chem Soc. 2013;135(34):12707–21.
49. Kang CS, Chen Y, Lee H, Liu D, Sun X, Kweon J, et al. Synthesis and evaluation of a new bifunctional NETA chelate for molecular targeted radiotherapy using90Y or177Lu. Nucl Med Biol. 2015;42(3):242–9.
50. McMurry TJ, Brechbiel M, Kumar K, Gansow OA. Convenient synthesis of bifunctional tetraaza macrocycles. Bioconjug Chem. 1992;3(2):108–17.
51. Wu C, Kobayashi H, Sun B, Yoo TM, Paik CH, Gansow OA, et al. Stereochemical influence on the stability of radio-metal complexes in vivo. Synthesis and evaluation of the four stereoisomers of 2-(p-nitrobenzyl)-trans-CyDTPA. Bioorg Med Chem. 1997;5(10):1925–34.
52. Hohloch K, Zinzani PL, Linkesch W, Jurczak W, Deptala A, Lorsbach M, et al. Radioimmunotherapy with 90Y-ibritumomab tiuxetan is a safe and efficient treatment for patients with B-cell lymphoma relapsed after auto-SCT: an analysis of the international RIT-Network. Bone Marrow Transplant. 2010;46(6):901–3.
53. Brechbiel MW, Gansow OA, Atcher RW, Schlom J, Esteban J, Simpson D, et al. Synthesis of 1-(p-isothiocyanatobenzyl) derivatives of DTPA and EDTA. Antibody labeling and tumor-imaging studies. Inorg Chem. 1986;25(16):2772–81.
54. Pauwels S, Barone R, Walrand S, Borson-Chazot F, Valkema R, Kvols LK, et al. Practical dosimetry of peptide receptor radionuclide therapy with 90Y-labeled somatostatin analogs. J Nucl Med. 2005;46(1 suppl):92S–8S.
55. Kunikowska J, Pawlak D, Bąk MI, Kos-Kudła B, Mikołajczak R, Królicki L. Long-term results and tolerability of tandem peptide receptor radionuclide therapy with 90Y/177Lu-DOTATATE in neuroendocrine tumors with respect to the primary location: a 10-year study. Ann Nucl Med. 2017;31(5):347–56.
56. Schneider DW, Heitner T, Alicke B, Light DR, McLean K, Satozawa N, et al. In vivo biodistribution, PET imaging, and tumor accumulation of 86Y- and 111In-antimindin/RG-1, engineered antibody fragments in LNCaP tumor-bearing nude mice. J Nucl Med. 2009;50(3):435–43.
57. Rösch F, Herzog H, Stolz B, Brockmann J, Köhle M, Mühlensiepen H, et al. Uptake kinetics of the somatostatin receptor ligand [86Y] DOTA-d Phe1-Tyr3-octreotide ([86Y]SMT487) using positron emission tomography in non-human primates and calculation of radiation doses of the 90Y-labelled analogue. Eur J Nucl Med Mol Imaging. 1999;26(4):358–66.
58. Salako QA, O'Donnell RT, DeNardo SJ. Effects of Radiolysis on Yttrium-90-Labeled Lym-1 Antibody Preparations. J Nucl Med. 1998;39(4):667–70.
59. Barone R, Walrand S, Konijnenberg M, Valkema R, Kvols LK, Krenning EP, et al. Therapy using labelled somatostatin analogues: comparison of the absorbed doses with 111In-DTPA-D-Phe1-octreotide and yttrium-labelled DOTA-D-Phe1-Tyr3-octreotide. Nucl Med Commun. 2008;29(3):283–90.